International Journal of Nanomedicine

Dovepress
open access to scientific and medical research

Open Access Full Text Article

ORIGINAL RESEARCH

Synthesis, characterization, and in vitro evaluation of curcumin-loaded albumin nanoparticles surface-functionalized with glycyrrhetinic acid

This article was published in the following Dove Press journal:
International Journal of Nanomedicine
27 August 2015
Number of times this article has been viewed

Jingjing Li[1]
Tong Chen[2]
Feng Deng[1]
Jingyuan Wan[1]
Yalan Tang[1]
Pei Yuan[1]
Liangke Zhang[1]

[1]Chongqing Medicine Engineering Research Center, Chongqing Key Laboratory of Biochemistry and Molecular Pharmacology, School of Pharmacy, Chongqing Medical University, Chongqing, [2]School of Pharmaceutical Sciences, Yunnan Key Laboratory of Pharmacology for Natural Products, Kunming Medical University, Kunming, People's Republic of China

Abstract: We have designed and developed curcumin (Ccn)-loaded albumin nanoparticles (BNPs) surface-functionalized with glycyrrhetinic acid (Ccn-BNP-GA) for GA receptor-mediated targeting. Ccn-BNP-GA was prepared by conjugating GA as a hepatoma cell-specific binding molecule onto the surface of BNPs. Ccn-BNP-GA showed a narrow distribution with an average size of 258.8±6.4 nm, a regularly spherical shape, an entrapment efficiency of 88.55%±5.54%, and drug loading of 25.30%±1.58%. The density of GA as the ligand conjugated to BNPs was 140.48±2.784 μg/g bovine serum albumin. Cytotoxicity assay results indicated that Ccn-BNP-GA was significantly more cytotoxic to HepG2 cells and in a concentration-dependent manner. Ccn-BNP-GA also appeared to be taken up to a greater extent by HepG2 cells than undecorated groups, which might be due to the high affinity of GA for GA receptors on the HepG2 cell surface. These cytotoxicity assay results were corroborated by analysis of cell apoptosis and the cell cycle. Further, Ccn-BNP-GA showed an approximately twofold higher rate of cell apoptosis than the other groups. Moreover, proliferation of HepG2 cells was arrested in G_2/M phase based on cell cycle analysis. These results, which were supported by the GA receptor-mediated endocytosis mechanism, indicate that BNPs surface-functionalized with GA could be used in targeted cancer treatment with high efficacy, sufficient targeting, and reduced toxicity.

Keywords: glycyrrhetinic acid, albumin, nanoparticles, surface-functionalized, curcumin

Introduction

Hepatocellular carcinoma is one of the most common human malignancies worldwide with high morbidity.[1] Chemotherapy is always the ubiquitous strategy for clinical treatment. However, current chemotherapeutic agents lack adequate selectivity and targeting efficacy.[1–3] Thus, novel drug delivery systems for the treatment of liver cancer need to be developed and investigated. Over the past few years, application of targeted drug delivery systems have been of considerable interest in disease management, especially active targeting.[4–6] Researchers have shown that surface functionalization of nanomaterials using glycyrrhetinic acid (GA) as a drug delivery targeting ligand was beneficial to the defined receptor recognition on the surface of hepatoma cells.[7–9] Generally, nanotechnology with preferred surface functionalization has the potential to improve the treatment of liver cancer.

Bovine serum albumin (BSA), characterized as a macromolecular protein carrier for drug delivery, is particularly interesting and is used widely because of its nontoxicity, non-immunogenicity,[10] and good biocompatibility.[11–13] Moreover, significant amounts

Correspondence: Liangke Zhang
Chongqing Medicine Engineering Research Center, Chongqing Key Laboratory of Biochemistry and Molecular Pharmacology, School of Pharmacy, Chongqing Medical University, District of Yuzhong, Chongqing 400016, People's Republic of China
Tel +86 23 6848 5161
Fax +86 23 6848 5161
Email zlkdyx@126.com

of drug can be encapsulated in the matrix, primarily because of the large number of drug-binding sites present in the albumin molecule.[14–16] As a consequence, BSA is a suitable nanocarrier for drug delivery, and is able to improve the solubility of lipophilic drugs and allow better controlled release.[17,18] Moreover, albumin nanoparticles (BNPs) provide multiple opportunities for surface functionalization because of the presence of functional carboxylic and amino groups on their surface.[19,20] In particular, conjugation of specific ligands to the surface of BNPs can be obtained by covalent binding. With regard to conjugation, a highly compatible and specific ligand is essential for active targeting, and should be able to bind selectively to a particular type of receptor on the target cells.[21]

Curcumin (Ccn), a hydrophobic polyphenol structure, is extracted from the rhizomes of *Curcuma longa*[22] and has a number of medicinal and therapeutic properties, including anti-inflammatory, antiseptic, antioxidative, and hypolipidemic effects.[23,24] Moreover, emerging evidence shows that Ccn might induce apoptosis or cell cycle arrest in several types of cancer. Non-cytotoxic to healthy cells,[25–27] Ccn can also serve as a drug or be an adjunct to traditional chemotherapy in the treatment of cancer.[28,29]

Given the aforementioned observations, the purpose of the present work was to develop Ccn-loaded BNPs surface-functionalized with GA (Ccn-BNP-GA) for GA receptor-mediated targeting. We examined the physicochemical properties of Ccn-BNP-GA and investigated its release in vitro. Further, the density of GA functionalization on the surface of the BNPs was evaluated by high-performance liquid chromatography (HPLC). The cellular uptake and cytotoxicity of Ccn-BNP-GA was also evaluated in vitro to validate its targeting potential in HepG2 cells. In addition, apoptosis and cell cycle arrest were determined by flow cytometry (FCM).

Materials and methods

Materials

The following materials were obtained from commercial suppliers and used as received. Ccn (98%), GA (98%), anhydrous dimethyl sulfoxide (DMSO), *N*-hydroxysuccinimide (NHS) and *N, N′*-dicyclohexyl carbodiimide (DCC) were obtained from Aladdin Industrial Corporation. BSA was sourced from Beijing Solarbio Science & Technology Co Ltd. Sephadex G-50 (Pharmacia) was provided by Shanghai Haoran Biological Technology Co Ltd. Roswell Park Memorial Institute (RPMI) 1640 medium and trypsin-ethylenediaminetetraacetic acid solution (0.25%) were obtained from Thermo Fisher Scientific Biological Chemical Co Ltd. MTT (tetrazolium salt) and DMSO were supplied by Biosharp Biotechnology Co Ltd. Penicillin and streptomycin solution were obtained from Beijing Dingguo Changsheng Biotechnology Co Ltd. Fetal bovine serum was supplied by Zhejiang Tianhang Biotechnology Co Ltd. Unless stated otherwise, all solvents were of analytical grade and sourced from Chengdu Kelong Chemical Co Ltd.

Preparation of Ccn-loaded albumin nanoparticles

Ccn-BNPs were prepared using a simple desolvation method.[30] In brief, the required amount of Ccn (4 mg) in ethanol (6 mL) was added dropwise to 10 mg of BSA in purified water (1 mL) at a rate of 1 mL/min under magnetic stirring. The coacervates thus formed were hardened under continued stirring for 4 hours under room conditions, followed by cross-linking with 0.5% glutaraldehyde (50 μL). After the scheduled reaction time, organic solvents were removed by a rotary evaporator at 35°C. The resultant nanoparticles were obtained. Blank BNPs were obtained as described earlier, except that ethanol without Ccn was added dropwise to the BSA solution for 4 hours.

Synthesis of GA-targeted albumin nanoparticles

The NHS ester of GA (GA-NHS)[31,32] was synthesized using the reported procedure to activate the functionality of GA. GA (1.0 g, 2.12 mmol) was dissolved in 20.0 mL of anhydrous DMSO, where 0.5 mL of triethylamine was added in advance. NHS (0.52 g, 4.52 mmol) and DCC (0.94 g, 4.56 mmol) were added and stirred ($mol_{GA}/mol_{NHS}/mol_{DCC}$ =1:2.13:2.15). The mixture was stirred further overnight at room temperature and filtered to remove the insoluble byproduct (dicyclohexylurea). The solution was mixed with diethyl ether, whereupon GA-NHS was precipitated, then washed repeatedly with anhydrous ether, and finally dried in a vacuum.

Ccn-BNP-GA was prepared as follows: 50 mg of GA-NHS in 0.5 mL of DMSO was slowly added to 3.5 mL of Ccn-BNP suspension. The mixture was stirred constantly for 1 hour. Ccn-BNP-GA was separated from the unreacted GA and other byproducts using the Sephadex G-50 column. Blank BNPs surface-functionalized with GA (BNP-GA) were also prepared as described previously, except that only GA-NHS solution was added dropwise to blank BNPs.

Characterization of the prepared nanoparticles

Entrapment efficiency (EE) and drug loading (DL) were determined by centrifugation at 14,000 rpm and 4.0°C for 30 minutes. The free drug in the supernatant was analyzed using an ultraviolet spectrophotometer (UV-2600, Shimadzu) at 430 nm. The EE and DL of the nanoparticles were calculated by Equations 1 and 2, respectively:

$$EE = \frac{\text{The amount of Ccn in the nanoparticles}}{\text{The amount of Ccn in the sample}} \times 100\% \quad (1)$$

$$DL = \frac{\text{The amount of Ccn in the nanoparticles}}{\text{The amount of nanoparticles}} \times 100\% \quad (2)$$

The thermal behavior of Ccn-BNPs and the physical state of Ccn were investigated using a differential scanning calorimeter. Samples of pure Ccn, pure BSA, physical mixture (Ccn-BSA), and Ccn-BNPs were properly sealed in an aluminum pan. Further, these samples were subjected to a thermal procedure using a heating rate of 10°C/min from 50°C to 300°C under nitrogen purge gas maintained at a flow rate of 20 mL/min. Samples were analyzed using a Netzsch STA449C thermal analyzer.

Fourier transform infrared spectroscopy

The structures of GA, BSA, GA-NHS, and BNP-GA were investigated using a Fourier transform infrared (FT-IR) spectrophotometer (Avatar 330, Thermo Nicolet) in the range of 4,000–400 cm^{-1}. All samples were mixed with KBr and pressed into pellets at ambient temperature, which were placed in the sample chamber of the FT-IR instrument for measurement. The scans were recorded by FT-IR spectra.

Quantification of GA to BSA conjugation ratio

Quantitative analysis of GA in BNP-GA was measured by HPLC (Shimadzu) to calculate the ratio of GA to BSA. BNP-GA was separated from the unreacted products using the Sephadex G-50 column and digested by 0.25% trypsin-ethylenediaminetetraacetic acid solution at 37°C. An HPLC system was used to determine the concentrations of GA in the samples. Chromatography was done using a LiChrospher RP C_{18} column (4.6 mm ×150 mm, 5 μm; Jiangsu Hanbon Science & Technology Co Ltd). The mobile phase was methanol/water/acetic acid (85:14.6:0.4, v/v).[33] The analysis was conducted at a flow rate of 1.0 mL/min at an absorbance of 251 nm.

Transmission electron microscopy and particle size

The morphology of Ccn-BNPs and Ccn-BNP-GA was visualized by transmission electron microscopy (TEM, H-7500, Hitachi Ltd). Samples were obtained by dropping appropriately diluted nanoparticles onto a carbon-coated 200 mesh copper grid to form a thin film. The film was stained, and the excess staining solution was removed with filter paper. The prepared grid was thoroughly air-dried prior to processing by TEM. The particle size and polydispersity index were examined using a Zetasizer (Malvern Instruments), and each sample was analyzed in triplicate.

In vitro drug release study

The in vitro release profiles for Ccn were estimated in phosphate-buffered saline (PBS; pH 7.4) by dialysis, with a molecular weight cut-off of 8,000–14,000 Da. First, 2.0 mL was added to a dialysis pocket, placed in 25 mL of PBS (pH 7.4), and incubated at 37°C with shaking at a speed of 100 rpm (n=3). The release medium (4 mL) was removed and replaced with 4 mL of fresh medium at predetermined time intervals. The amount of Ccn in the release medium was evaluated using an ultraviolet-visible spectrophotometer (UV-2600, Shimadzu) at 430 nm. Each experiment was conducted in triplicate, and the results are presented as the mean ± standard deviation (SHZ-88, Jiangsu Taichang Co Ltd).

Cell culture

The hepatocellular carcinoma (HepG2) cell line was supplied by Chongqing Key Laboratory of Biochemistry and Molecular Pharmacology and cultivated in RPMI 1640 medium supplemented with 10% fetal bovine serum and 1% penicillin-streptomycin solution at 37°C in a fully humidified incubator maintained with 5% CO_2. When the cells covered 70%–80% of the bottom of a T-25 flask, the cell medium was removed and the cells were flushed with PBS twice. The cells were then incubated with trypsin-ethylenediaminetetraacetic acid solution (0.25%) to detach them from the flask. The trypsin was neutralized by adding RPMI 1640 medium supplemented with 10% fetal bovine serum. The cell suspension was centrifuged at 1,000 rpm for 5 minutes and then put into new flasks with fresh medium. No ethics statement was required from the institutional review board for the use of this cell line.

In vitro cell cytotoxicity assay

Cytotoxicity was assessed by MTT assay as described elsewhere.[34,35] Cells (5×10^3/well) were seeded in 96-well plates with 100 μL/well and cultured for attachment in RPMI 1640

medium with 10% fetal bovine serum at 37°C in an incubator with 5% CO_2 and 95% air. When the cells reach 70%–80% confluence with normal morphology, they were treated with Ccn-loaded formulations in concentrations of 27.15, 54.29, 81.44, 108.58, and 135.73 μmol/L. Untreated cells were used as the control (with 100% cell viability), and the medium without addition of cells was used as the blank. After incubation for a predetermined time, 20 μL of MTT solution (5 mg/mL in PBS) was added to each well and the cells were further incubated at 37°C for 24 hours. Finally, the culture medium was removed and 150 μL of DMSO was added under gentle shaking for 10 minutes to dissolve the formazan crystals. Absorbance was determined using a Bio-Tek ELx800 Quant Universal microplate spectrophotometer at 570 nm. Cytotoxicity was determined by calculating Equation 3, as follows:

$$\text{Cytotoxicity (\%)} = \frac{OD_{control/570nm} - OD_{sample/570nm}}{OD_{control/570nm} - OD_{blank/570nm}} \times 100\% \quad (3)$$

We conducted a competitive binding experiment to investigate the specific interaction between the nanocarriers and GA receptors on tumor cells, as follows. HepG2 cells were routinely incubated at 37°C for attachment. The medium was replaced with 135.73 μmol/L free GA to block the GA receptors for 2 hours prior to application of Ccn-BNP-GA. The HepG2 cells were then rinsed three times with PBS and treated with Ccn-BNP-GA for a further 24 hours to observe its cytotoxic effects. The subsequent procedure was similar to the aforementioned methods in the cell cytotoxicity assay. At the same time, the images were observed using an inverted microscope to detect the cell morphology.

In vitro cellular uptake

HepG2 cells (5×10^4 cells/well) were cultured in six-well plates with RPMI 1640 medium to quantify the cellular uptake. Cells were treated with Ccn suspension, Ccn-BNPs, and Ccn-BNP-GA at a drug concentration of 135.73 μmol/L for 4 hours. After incubation, the cells were collected and kept in 200 μL of ultrapure water at −80°C more than three times. After centrifugation (at 14,000 rpm for 15 minutes), 1.5 mL of ethyl acetate was added to 200 μL of the supernatant and vortexed. After centrifugation, the supernatant was dried in a vacuum. Aliquots of the samples were injected into a Hypersil™ BDS C_{18} column (15 cm ×4.5 mm ×5 μm; Dalian Elite Analytical Instruments Co Ltd). The mobile phase was methanol/water/citric acid (73:26.7:0.3).[30] The flow rate was 1.0 mL/min, and the amount of Ccn present was analyzed using an ultraviolet-visible detector at 430 nm.

We conducted a competitive binding experiment to determine if GA receptors specifically mediated the cellular uptake of Ccn encapsulated in Ccn-BNP-GA. HepG2 cells (5×10^4 cells/well) was propagated in six-well plates. After reaching subconfluence in the six-well plates, the attached cells were exposed to 135.73 μmol/L free GA for 2 hours. The cells were then treated with Ccn-BNP-GA for a further 4 hours. The subsequent process is the same as that mentioned in the cellular uptake assay.

Assessment of apoptosis and cell cycle by FCM

A detection kit containing Annexin V-fluorescein isothiocyanate and propidium iodide (PI), which determines translocation of phosphatidylserine to the cell surface, was utilized to quantify the amount of apoptotic cells. First, 5×10^4 HepG2 cells were allowed to adhere in six-well plates. After exposure to Ccn suspension, Ccn-BNPs, or Ccn-BNP-GA for 24 hours, the apoptotic and live cells were harvested by centrifugation (at 1,000 rpm for 5 minutes). Cells in the sediment were then resuspended in 1.5 mL of PBS and stained with Annexin V-fluorescein isothiocyanate and PI according to the manufacturer's instructions. The number of apoptotic cells was monitored by measuring the fluorescence of the cells with an FCM instrument (BD FACS Vantage SE). Live, early apoptotic, late apoptotic, and necrotic cells are designated as Z_1, Z_2, Z_3, and Z_4, respectively.

For analysis of the cell cycle, the drug-treated cells were washed, collected by centrifugation (1,000 rpm, 5 minutes), fixed in chilled 70% ethanol, and labeled with PI and RNase. The samples were analyzed by FCM (BD FACS Vantage SE).

A competitive binding experiment was also performed, which involved preincubation of 135.73 μmol/L free GA for 2 hours, with addition of Ccn-BNP-GA to each well at a predetermined time point. The subsequent procedure was the same as that as described in the assessment of apoptosis and cell cycle.

Statistical analysis

The study data are expressed as the mean ± standard deviation. All statistical evaluations of data were conducted using Statistical Package for the Social Sciences version 18.0 software.

Results and discussion

Synthesis and characterization of nanoparticles

Measuring the quantity of GA to BSA conjugation is critical for efficient targeted delivery. The more surface

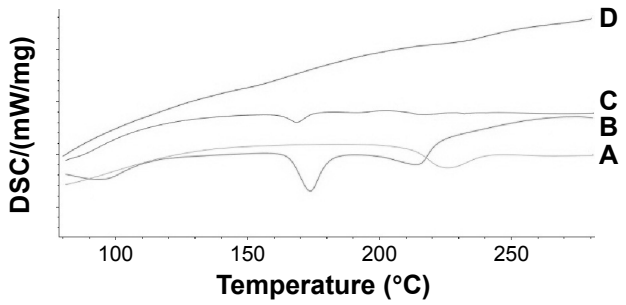

Figure 1 Differential scanning calorimetry for reagents.
Notes: (**A**) Bovine serum albumin, (**B**) physical mixture, (**C**) curcumin, and (**D**) curcumin-loaded albumin nanoparticles.
Abbreviation: DSC, differential scanning calorimetry.

functionalization by GA, the higher affinity the Ccn-BNP-GA may have through GA receptor-mediated endocytosis. BNPs significantly enable access to functionalization on the primary amino or carboxylic groups into other functional groups.[19,20] BNPs were prepared using the desolvation method. The amino groups on the surface of Ccn-BNPs were covalently bound by dropwise addition of GA-NHS. As a result, Ccn-BNP-GA was prepared based on the two steps described previously. The quantitative binding ratio of GA to BSA estimated by HPLC was 140.48±2.784 μg/g BSA.

The differential scanning calorimetry curves are shown in Figure 1. BSA exhibited a thermal event attributable to BSA melting with an onset at 215°C and a peak temperature of 225°C. In the endothermic curve of the Ccn/BSA physical mixture, the peak temperature of Ccn/BSA was observed at approximately 175°C and 225°C. Pure Ccn showed an endothermic transition at 175°C related to the melting point. Given that Ccn was entrapped in BSA, no peak temperature in the curve of Ccn-BNPs, which indicates that crystallization of Ccn was inhibited by albumin during preparation of the BNPs, was observed, unlike the thermal behavior observed for the physical mixture of Ccn/BSA.

The surface-functionalized groups were then observed by FT-IR spectroscopy, as shown in Figure 2, to identify the probable associations between BNPs and GA. As shown in the figure, raw GA was characterized by peaks at 1,654, 1,729, and 3,434 cm^{-1}, which were attributed to C=O and O–H bending vibrations. The structure of oleanane pentacyclic triterpenoids was indicated by the spectral signatures at 1,387 and 1,364 cm^{-1} because of the C–H bending vibration at the C_4 position. The absorption bands at 2,960 and 2,866 cm^{-1} corresponded to C-CH_3 absorption and aliphatic C-H stretching. The peak intensities at 1,467, 1,392, and 1,085 cm^{-1} were attributed to the CH_2, CH_3, and C-O deformation vibrations, respectively. Considering BSA with a large number of amino bonds, evident absorption peaks of N-H bending were observed at 1,659 and 3,391 cm^{-1}. The other major absorption peaks between 2,945 cm^{-1} and 2,868 cm^{-1} were ascribed to C–H stretching. Further, the characteristic absorption peaks of GA-NHS in the 1,741 and 1,651 cm^{-1} regions corresponded to C=O stretching vibration. Meanwhile, the peak intensity at 1,741 cm^{-1} decreased with the disappearance of the carboxylic group. For BNP-GA, the peak at 3,371 cm^{-1} broadened, which corresponded to O-H and N-H stretching and formation of strong intermolecular and intramolecular H-bonding. The absorption of the amide band I at 1,649 cm^{-1}, amide band II at 1,559 cm^{-1},

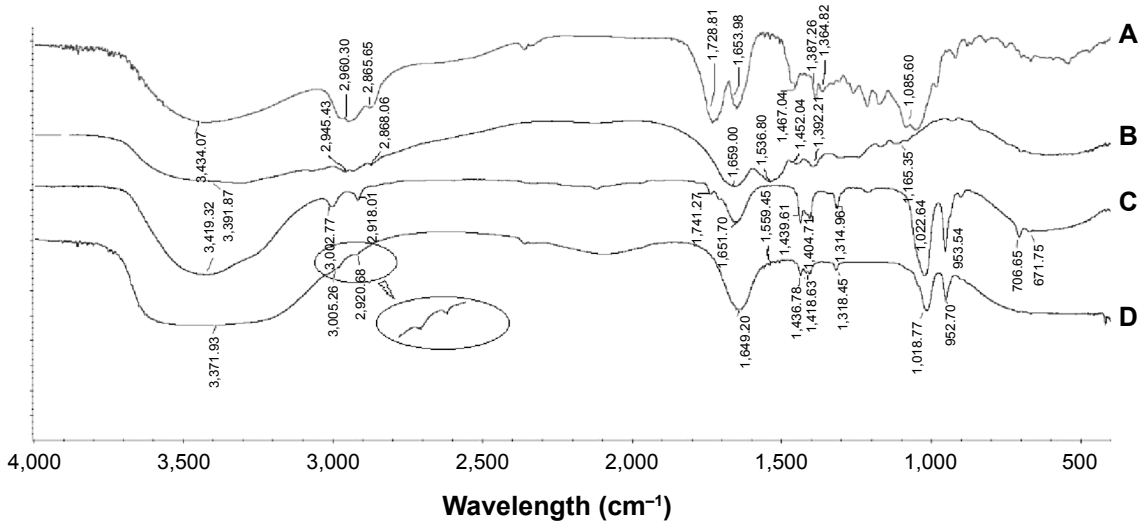

Figure 2 Fourier transform infrared spectra for reagents.
Notes: (**A**) GA, (**B**) bovine serum albumin, (**C**) *N*-hydroxysuccinimide ester of GA, and (**D**) albumin nanoparticles surface-functionalized with GA.
Abbreviation: GA, glycyrrhetinic acid.

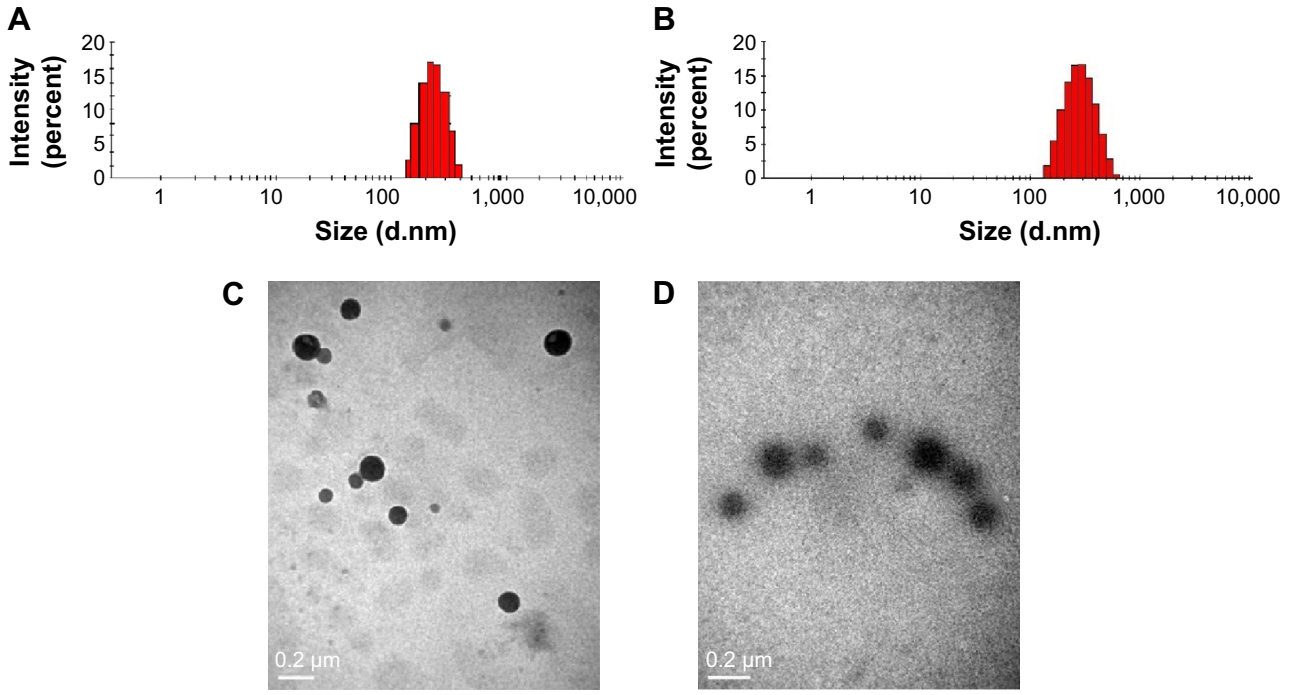

Figure 3 Transmission electron micrographs and size distribution of curcumin-loaded albumin nanoparticles (**A**, **C**) and curcumin-loaded albumin nanoparticles surface-functionalized with GA (**B**, **D**).
Abbreviation: GA, glycyrrhetinic acid.

and amide band III at 1,318 cm^{-1} were the characteristic peaks, indicating that some specific interactions occurred between the carboxylic group of GA and the amino group of BSA. Moreover, some subtle changes were observed, ie, the intensity at 1,649 cm^{-1} became sharper and the vibration at 1,559 cm^{-1} receded markedly when compared with the spectrum for BSA. In addition, the peak of the carboxylic group in GA completely disappeared. The aforementioned results imply that GA was successfully conjugated onto the surface of the BNPs.

Figure 3 shows the size distribution and representative TEM images of the nanoparticles. The particle size of Ccn-BNP-GA was 258.8±6.4 nm, which differed from that of Ccn-BNPs (225.5±3.8 nm). Only a subtle variation was observed, and the size was not markedly altered by GA functionalization. Further, the nanoparticles exhibited a spherical-shaped morphology.

EE and DL are also fundamental properties of nanoparticles to consider when devising a targeted drug delivery system. Table 1 shows that the EEs of Ccn-BNPs and Ccn-BNP-GA were 84.87%±3.38% and 88.55%±5.54%, respectively. The DL of Ccn-BNP and Ccn-BNP-GA was 24.25%±0.96% and 25.30%±1.58%, respectively. Polydispersity index values were slightly lower than 0.3, indicating a narrow distribution.

Purification by Sephadex gel chromatography

GA was coupled with the amino groups of the BNPs by covalent bonding. BNP-GA was prepared and segregated from the unreacted GA using the Sephadex G-50 column. Trypsin was used to enzymolyse the obtained samples. Figure 4 shows the elution curve of the ultraviolet-visible spectrum of absorption at 251 nm. The two peaks appear to denote BNP-GA and the unreacted substrate, respectively. As a result, BNP-GA was completely separated from the unreacted GA.

In vitro release properties

The in vitro release profiles for Ccn from Ccn suspension, Ccn-BNPs, and Ccn-BNP-GA in PBS solution (pH 7.4) are

Table 1 Basic characterization of nanoparticles

	Particle size (nm)	PDI	EE (%)	DL (%)
Ccn-BNPs	225.5±3.8	0.073±0.033	84.87±3.38	24.25±0.96
Ccn-BNP-GA	258.8±6.4	0.111±0.019	88.55±5.54	25.30±1.58

Abbreviations: EE, entrapment efficiency; DL, drug loading; GA, glycyrrhetinic acid; PDI, polydispersity index; Ccn-BNP-GA, curcumin-loaded albumin nanoparticles surface-functionalized with GA; Ccn-BNPs, curcumin-loaded albumin nanoparticles.

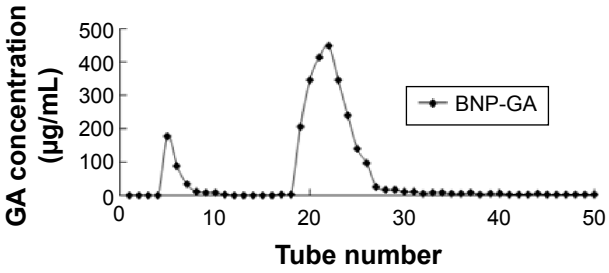

Figure 4 Flow curve on a Sephadex-50 column.
Abbreviations: BNP, albumin nanoparticle; GA, glycyrrhetinic acid.

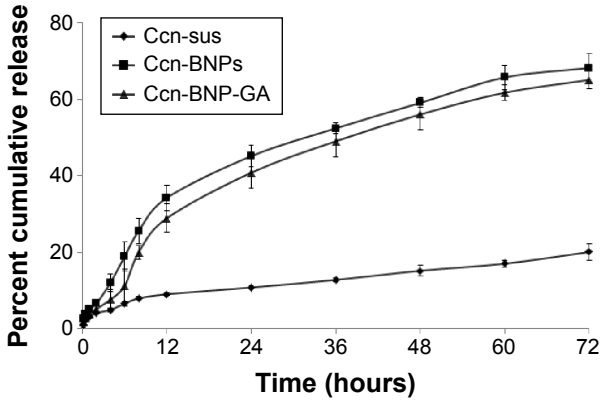

Figure 5 In vitro release profiles of Ccn-sus, Ccn-BNPs, and Ccn-BNP-GA.
Abbreviations: Ccn-sus, curcumin suspension; Ccn-BNPs, curcumin-loaded albumin nanoparticles; Ccn-BNP-GA, curcumin-loaded albumin nanoparticles surface-functionalized with GA; GA, glycyrrhetinic acid.

shown in Figure 5. First, the Ccn suspension used as the control was released slowly at a steady speed, where the amount of release was 20.13% and continued for 72 hours. In contrast, Ccn-BNPs and Ccn-BNP-GA showed a faster release based on addition of water-soluble material. After a burst release for up to 12 hours in the initial stage, Ccn-BNPs and Ccn-BNP-GA showed a prolonged and slow release pattern at a constant rate over 72 hours.

In vitro cytotoxicity assays

As shown in Figure 6, when the Ccn-loaded formulations at various concentrations were added to the incubated cells for 24 hours, a dramatic decrease in cell viability could be observed. The anticancer activity of Ccn-BNP-GA was significantly higher than that of the other formulations, which could be ascribed to GA receptor-mediated specific endocytosis. Moreover, a competitive binding assay was conducted by adding free GA prior to application of Ccn-BNP-GA. The inhibition rate gradually manifested a decreased pattern, and the results revealed that free GA competed with Ccn-BNP-GA to bind with GA receptors on the HepG2 cell surface, thus leading to saturation of GA receptors and inhibiting the delivery of Ccn-BNP-GA into cells. Generally, more Ccn-BNP-GA was internalized by GA receptor-mediated endocytosis than undecorated Ccn-BNPs,

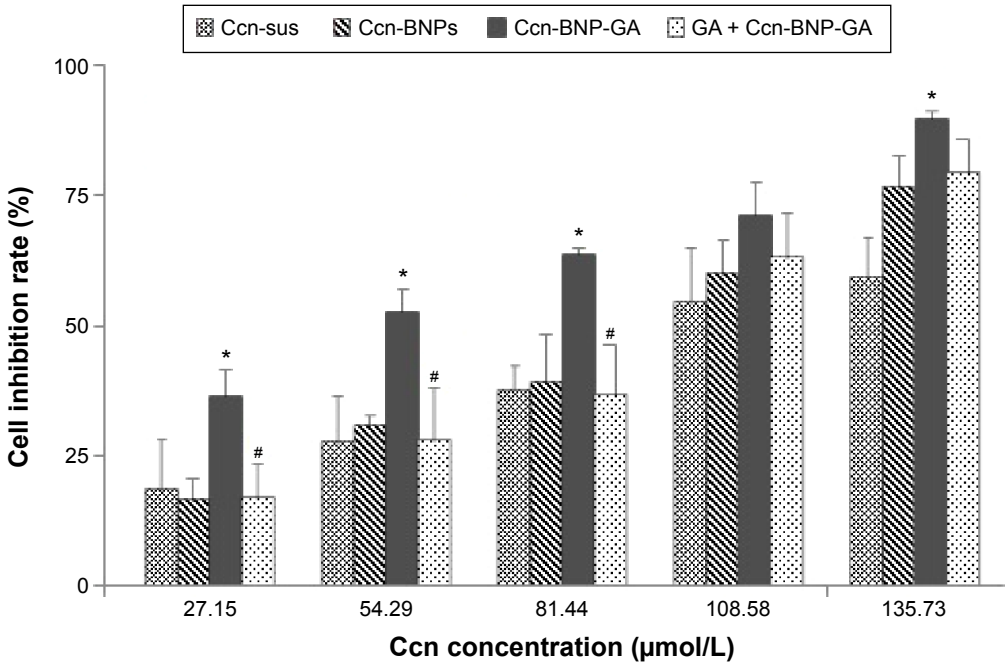

Figure 6 In vitro cytotoxicity of Ccn-sus, Ccn-BNPs, Ccn-BNP-GA, and GA + Ccn-BNP-GA against HepG2 cells for 24 hours.
Notes: Each point represents the mean ± standard deviation (n=6). *$P<0.05$ compared with Ccn-BNPs, #$P<0.05$ compared with Ccn-BNP-GA.
Abbreviations: Ccn-sus, curcumin suspension; Ccn-BNPs, curcumin-loaded albumin nanoparticles; Ccn-BNP-GA, curcumin-loaded albumin nanoparticles surface-functionalized with GA; GA, glycyrrhetinic acid.

and the Ccn-loaded formulations inhibited HepG2 cells in a concentration-dependent manner.

Figure 7 shows photographs of HepG2 cells treated with Ccn-loaded formulations. Compared with the control, HepG2 cells became smaller in Ccn-BNP-GA. However, some live cells with spindle-shaped adherent growth were observed in the competitive binding assay, indicating that the cell inhibition rate decreased. The observed number of apoptotic cells was basically consistent with the cytotoxicity seen over the observation period of 24 hours.

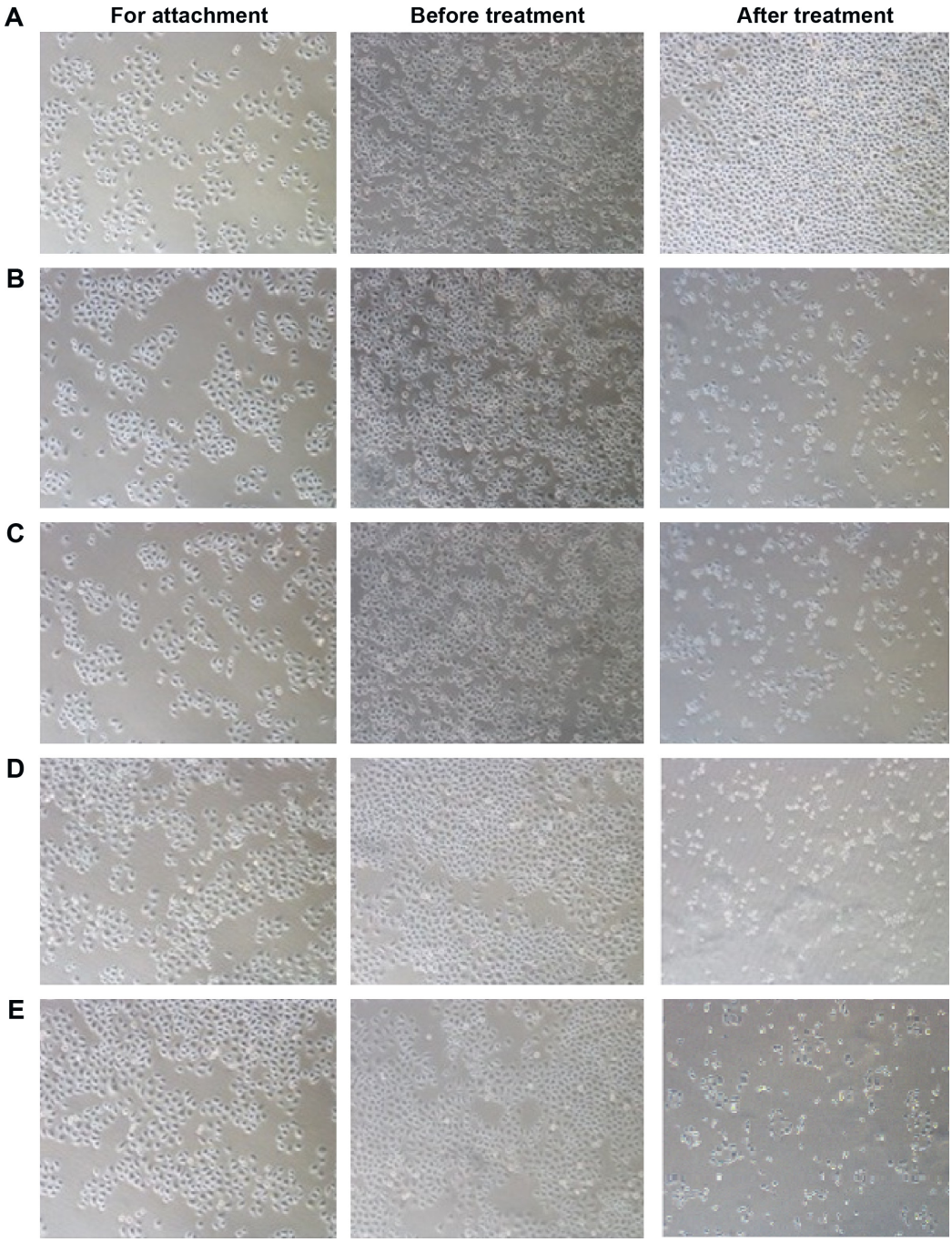

Figure 7 Photographs of HepG2 cells treated with curcumin suspension, curcumin-loaded albumin nanoparticles, curcumin-loaded albumin nanoparticles surface-functionalized with GA, and GA + curcumin-loaded albumin nanoparticles surface-functionalized with GA for 24 hours.
Notes: (**A**) Control; (**B**) Ccn-sus; (**C**) Ccn-BNPs; (**D**) Ccn-BNP-GA; (**E**) GA+Ccn-BNP-GA.
Abbreviations: Ccn-sus, curcumin suspension; Ccn-BNPs, curcumin-loaded albumin nanoparticles; Ccn-BNP-GA, curcumin-loaded albumin nanoparticles surface-functionalized with GA; GA, glycyrrhetinic acid.

In vitro cellular uptake

In this study, HPLC was used to measure intracellular drug concentrations and to detect whether the Ccn-loaded formulations could be endocytosed into HepG2 cells. As shown in Figure 8, the amounts of intracellular Ccn of Ccn suspension and Ccn-BNPs were 52.22±11.04 ng/10^5 cells and 56.10±11.57 ng/10^5 cells, respectively. However, Ccn-BNP-GA achieved a significantly higher drug concentration than non-conjugated nanoparticles probably because of the strong binding interactions between GA and its receptors. Further, we conducted a competitive binding experiment with addition of free GA in advance. As a consequence, the concentrations of Ccn decreased significantly in contrast with the groups without free GA. The presence of free GA as an inhibitor hindered the binding of GA to its receptors. The cell uptake results showed that Ccn-BNP-GA could be actively targeted to GA-positive cells.

Apoptosis and cell cycle assessed by FCM

Apoptosis was determined using the Annexin V-fluorescein isothiocyanate detection kit to further validate the potential of Ccn-BNP-GA as a drug delivery agent specific for GA-positive cells. In Figure 9, Z_1, Z_2, Z_3, and Z_4 denote viable cells, early apoptotic cells, late apoptotic cells, and necrotic cells, respectively. The apoptosis rate is the total of Z_2 and Z_3. FCM with Annexin V-PI staining revealed that the apoptosis rate increased from 6.49% in the control group to 66.65% in the Ccn-BNP-GA group. The apoptosis rate for Ccn-BNP-GA was approximately twofold higher than that of Ccn suspension and Ccn-BNPs. As shown in Figure 9B and 9C, the proportion of viable cells decreased from 63.85% in the Ccn suspension group to 54.89% in the Ccn-BNP group, and the proportion of apoptotic cells were increased slightly from 35.82% to 45.00%. A competitive binding experiment was also conducted, and the results revealed that the apoptotic cells was gradually reduced by 35.12% when compared with Ccn-BNP-GA. These observations infer that Ccn-BNP-GA preferentially targeted GA receptors on the HepG2 cells.

The FCM procedure (BD FACS Vantage SE) was used to further analyze how the involvement of Ccn-BNP-GA changed the distribution of HepG2 cells present in different phases of the cell cycle. As seen in Figure 10, treatment of HepG2 cells with the Ccn suspension led to a gradual increment in G_2/M phase cells compared with the control. Moreover, treatment with Ccn-BNPs or Ccn-BNP-GA resulted in changes ranging from 9.59% to 14.12% in G_2/M phase; Ccn-BNP-GA differed from the control group by 4.52% and the Ccn suspension group by 6.88%. Further, a dramatic decrease in the G_2/M phase was observed in the competitive binding experiment. These data confirm that Ccn-BNP-GA can induce cell cycle arrest in the G_2/M phase.

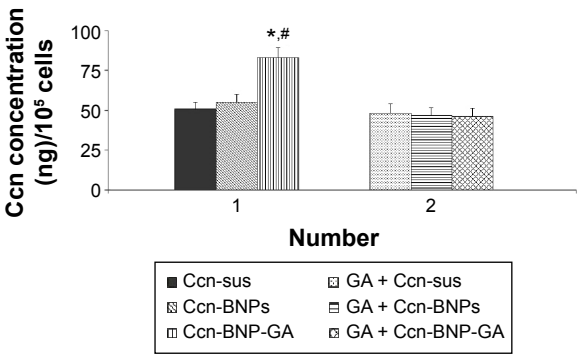

Figure 8 Effect of free GA on the ability of Ccn-BNP-GA to bind to HepG2 cells over 24 hours.

Notes: *$P<0.05$ compared with Ccn-sus, #$P<0.05$ compared with free GA + Ccn-BNP-GA. The results are expressed as the mean ± standard deviation (n=3).

Abbreviations: Ccn-sus, curcumin suspension; Ccn-BNPs, curcumin-loaded albumin nanoparticles; Ccn-BNP-GA, curcumin-loaded albumin nanoparticles surface-functionalized with GA; GA, glycyrrhetinic acid.

Conclusion

In this study, Ccn-BNP-GA was successfully prepared and characterized. The average size of Ccn-BNP-GA was 258.8±6.4 nm, with a narrow size distribution. Satisfactory EE and DL were also obtained. The targeting ability and effects of Ccn-BNP-GA were determined based on cytotoxicity, cellular uptake, apoptosis, and the cell cycle. All of the results validate that Ccn-BNP-GA could be a potentially effective targeted therapy agent for GA-positive tumor cells in vitro, which may help us elucidate the mechanism of GA receptor-mediated endocytosis. In conclusion, BNPs surface-functionalized with GA may be a promising therapeutic option for the treatment of hepatocellular carcinoma.

Acknowledgments

This project was supported by the Natural Science Foundation Project of CQ CSTC (cstc2012jjA10021), the National Research Foundation for the Doctoral Program of Higher Education of China (20125503120003), the Chongqing Board of Health Project (2013-2-060), and the Students' Research and Innovation Experimental Project of Chongqing Medical University (201432, 201244).

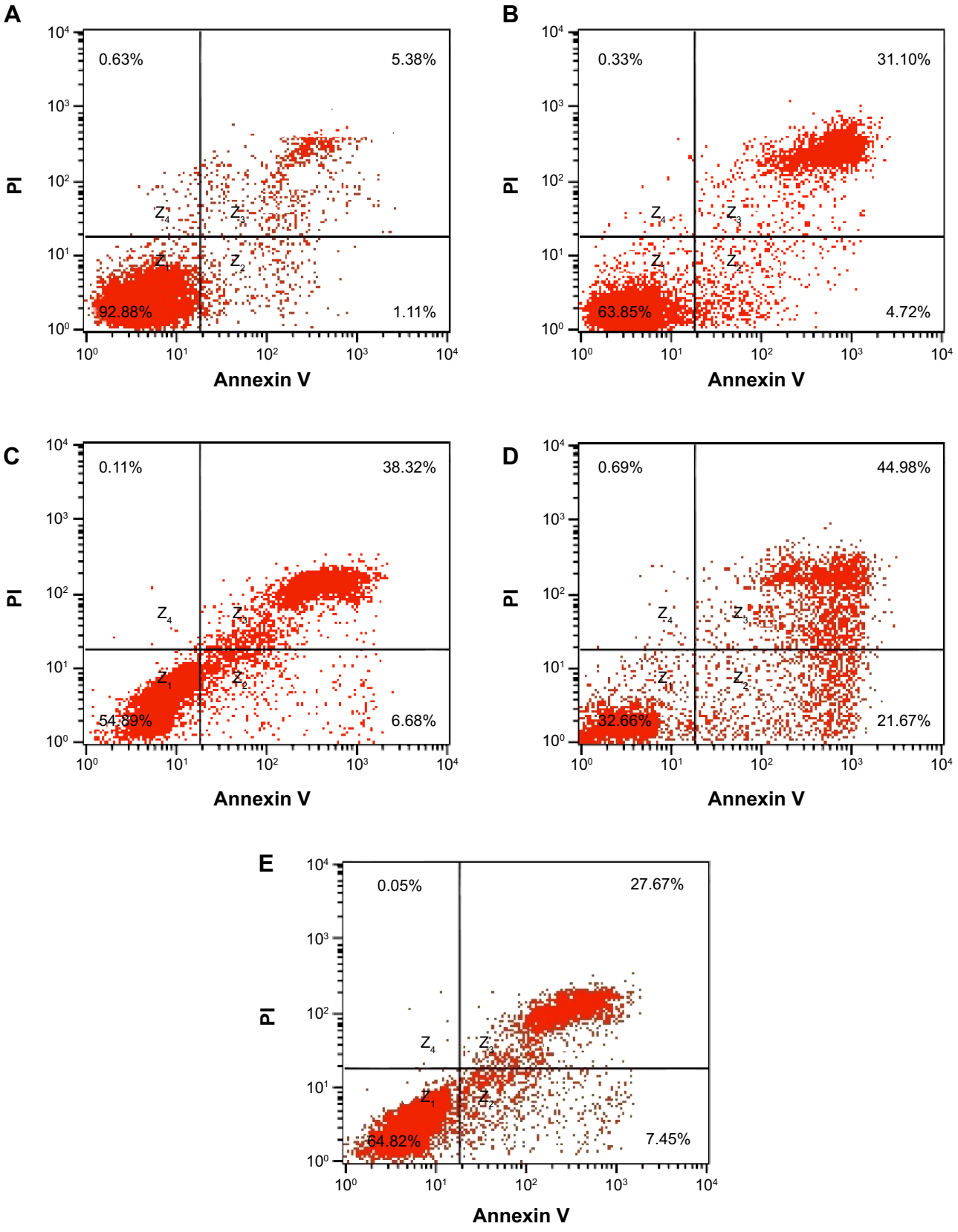

Figure 9 Effect of curcumin-induced apoptosis in HepG2 cells exposed to various formulations for 24 hours.
Notes: (**A**) Control, (**B**) curcumin suspension, (**C**) curcumin-loaded albumin nanoparticles, (**D**) curcumin-loaded albumin nanoparticles surface-functionalized with GA, and (**E**) GA + curcumin-loaded albumin nanoparticles surface-functionalized with GA.
Abbreviations: GA, glycyrrhetinic acid; PI, propidium iodide.

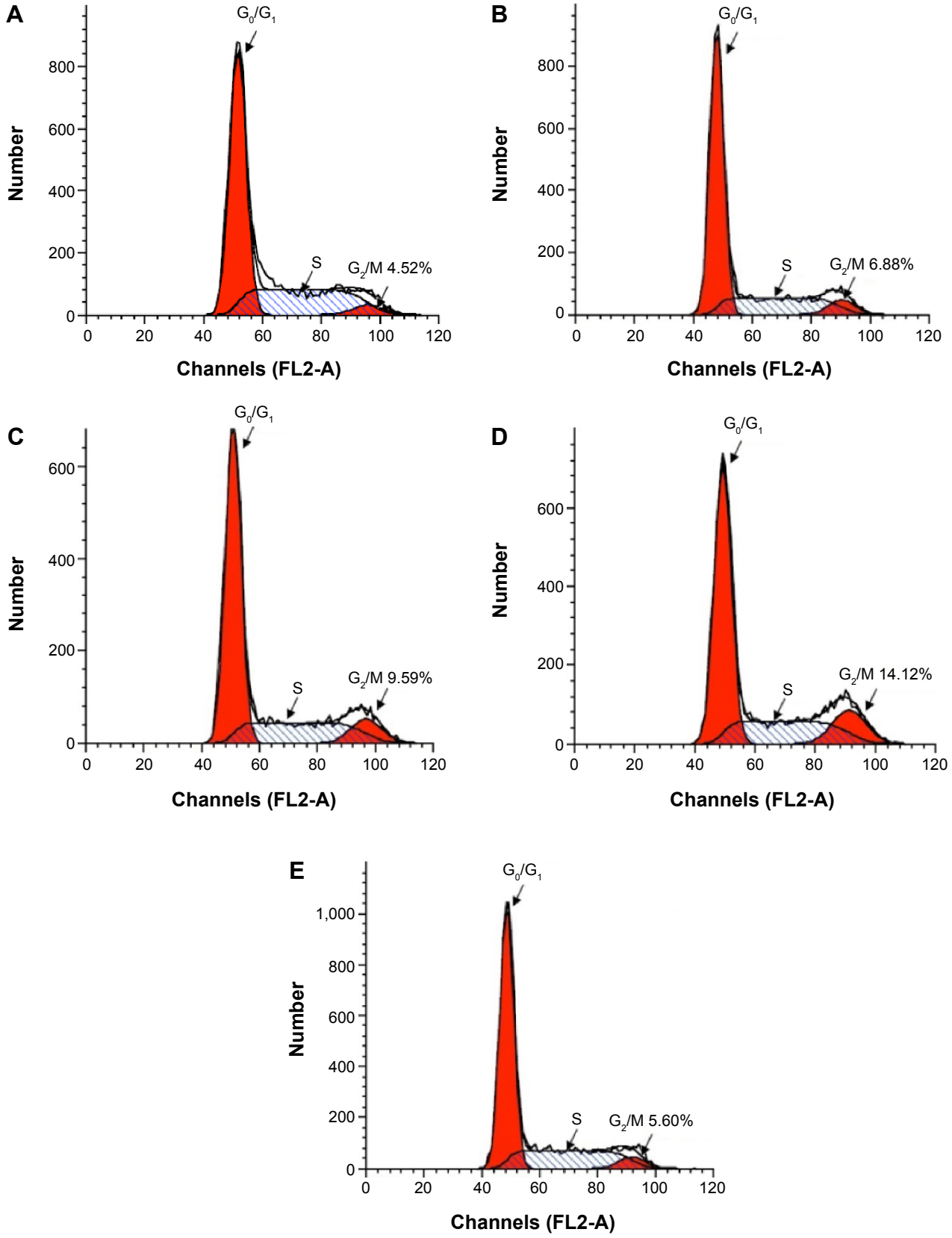

Figure 10 Effect of 24 hours of treatment with curcumin on the cell cycle in HepG2 cells.
Notes: (**A**) Control, (**B**) curcumin suspension, (**C**) curcumin-loaded albumin nanoparticles, (**D**) curcumin-loaded albumin nanoparticles surface-functionalized with GA, and (**E**) GA + curcumin-loaded albumin nanoparticles surface-functionalized with GA.
Abbreviation: GA, glycyrrhetinic acid.

Disclosure

The authors report no conflicts of interest in this work.

References

1. Liao YT, Liu CH, Yu J, Wu KC. Liver cancer cells: targeting and prolonged-release drug carriers consisting of mesoporous silica nanoparticles and alginate microspheres. *Int J Nanomedicine*. 2014;9:2767–2778.
2. Hu CM, Zhang L. Nanoparticle-based combination therapy toward overcoming drug resistance in cancer. *Biochem Pharmacol*. 2012;83(8):1104–1111.
3. Zhang X, Guo S, Fan R, et al. Dual-functional liposome for tumor targeting and overcoming multidrug resistance in hepatocellular carcinoma cells. *Biomaterials*. 2012;33(29):7103–7114.
4. Zhang XJ, Zhang XG, Yu PE, Han YC, Li YG, Li CX. Hydrotropic polymeric mixed micelles based on functional hyperbranched polyglycerol copolymers as hepatoma-targeting drug delivery system. *J Pharm Sci*. 2013;102(1):145–153.
5. Xun S, Fang W, Wei L, Zhang ZR. Sustained-release hydroxycamptothecin polybutylcyanoacrylate nanoparticles as a liver targeting drug delivery system. *Pharmazie*. 2004;59(10):791–794.
6. Cheng M, Gao X, Wang Y, et al. Synthesis of liver-targeting dual-ligand modified GCGA/5-FU nanoparticles and their characteristics in vitro and in vivo. *Int J Nanomedicine*. 2013;8:4265–4276.
7. Mao SJ, Bi YQ, Jin H, Wei DP, He R, Hou SX. Preparation, characterization and uptake by primary cultured rat hepatocytes of liposomes surface-modified with glycyrrhetinic acid. *Pharmazie*. 2007;62(8):614–619.
8. Huang W, Wang W, Wang P, et al. Glycyrrhetinic acid-modified poly(ethylene glycol)-b-poly(gamma-benzyl l-glutamate) micelles for liver targeting therapy. *Acta Biomater*. 2010;6(10):3927–3935.
9. Zhang C, Wang W, Liu T, et al. Doxorubicin-loaded glycyrrhetinic acid-modified alginate nanoparticles for liver tumor chemotherapy. *Biomaterials*. 2012;33(7):2187–2196.
10. Zhao D, Zhao X, Zu Y, et al. Preparation, characterization, and in vitro targeted delivery of folate-decorated paclitaxel-loaded bovine serum albumin nanoparticles. *Int J Nanomedicine*. 2010;5:669–677.
11. Langer K, Balthasar S, Vogel V, Dinauer N, von Briesen H, Schubert D. Optimization of the preparation process for human serum albumin (HSA) nanoparticles. *Int J Pharm*. 2003;257(1–2):169–180.
12. Kommareddy S, Amiji M. Preparation and evaluation of thiol-modified gelatin nanoparticles for intracellular DNA delivery in response to glutathione. *Bioconjug Chem*. 2005;16(6):1423–1432.
13. Azarmi S, Tao X, Chen H, et al. Formulation and cytotoxicity of doxorubicin nanoparticles carried by dry powder aerosol particles. *Int J Pharm*. 2006;319(1–2):155–161.
14. Elzoghby AO, Samy WM, Elgindy NA. Albumin-based nanoparticles as potential controlled release drug delivery systems. *J Control Release*. 2012;157(2):168–182.
15. Zu YG, Zhang Y, Zhao XH, Zhang Q, Liu Y, Jiang R. Optimization of the preparation process of vinblastine sulfate (VBLS)-loaded folate-conjugated bovine serum albumin (BSA) nanoparticles for tumor-targeted drug delivery using response surface methodology (RSM). *Int J Nanomedicine*. 2009;4:321–333.
16. Miele E, Spinelli GP, Miele E, Tomao F, Tomao S. Albumin-bound formulation of paclitaxel (Abraxane (R) ABI-007) in the treatment of breast cancer. *Int J Nanomedicine*. 2009;4(1):99–105.
17. Jain D, Banerjee R. Comparison of ciprofloxacin hydrochloride-loaded protein, lipid, and chitosan nanoparticles for drug delivery. *J Biomed Mater Res B Appl Biomater*. 2008;86(1):105–112.
18. Arnedo A, Irache JM, Merodio M, Espuelas Millan MS. Albumin nanoparticles improved the stability, nuclear accumulation and anticytomegaloviral activity of a phosphodiester oligonucleotide. *J Control Release*. 2004;94(1):217–227.
19. Ulbrich K, Hekmatara T, Herbert E, Kreuter J. Transferrin- and transferrin-receptor-antibody- modified nanoparticles enable drug delivery across the blood-brain barrier (BBB). *Eur J Pharm Biopharm*. 2009;71(2):251–256.
20. Steinhauser IM, Langer K, Strebhardt KM, Spankuch B. Effect of trastuzumab-modified antisense oligonucleotide-loaded human serum albumin nanoparticles prepared by heat denaturation. *Biomaterials*. 2008;29(29):4022–4028.
21. Wilson B, Ambika TV, Patel RDK, Jenita JL, Priyadarshini SRB. Nanoparticles based on albumin: preparation, characterization and the use for 5-flurouracil delivery. *Int J Biol Macromol*. 2012;51(5):874–878.
22. Qian H, Yang Y, Wang X. Curcumin enhanced adriamycin-induced human liver-derived hepatoma G2 cell death through activation of mitochondria-mediated apoptosis and autophagy. *Eur J Pharm*. 2011;43(3):125–131.
23. Cao J, Liu Y, Jia L, et al. Curcumin induces apoptosis through mitochondrial hyperpolarization and mtDNA damage in human hepatoma G2 cells. *Free Radic Biol Med*. 2007;43(6):968–975.
24. Wang M, Ruan YX, Chen QA, Li SP, Wang QL, Cai JY. Curcumin induced HepG2 cell apoptosis-associated mitochondrial membrane potential and intracellular free Ca2+ concentration. *Eur J Pharmacol*. 2011;650(1):41–47.
25. Syng-ai C, Kumari AL, Khar A. Effect of curcumin on normal and tumor cells: Role of glutathione and bcl-2. *Mol Cancer Ther*. 2004;3(9):1101–1108.
26. Kunwar A, Barik A, Mishra B, Rathinasamy K, Pandey R, Priyadarsini KI. Quantitative cellular uptake, localization and cytotoxicity of curcumin in normal and tumor cells. *Biochim Biophys Acta*. 2008;1780(4):673–679.
27. Hatcher H, Planalp R, Cho J, Tortia FM, Torti SV. Curcumin: from ancient medicine to current clinical trials. *Cell Mol Life Sci*. 2008;65(11):1631–1652.
28. Kumar V, Lewis SA, Mutalik S, Shenoy DB, Venkatesh, Udupa N. Biodegradable microspheres of curcumin for treatment of inflammation. *Indian J Physiol Pharmacol*. 2002;46(2):209–217.
29. Fan H, Tian W, Ma X. Curcumin induces apoptosis of HepG2 cells via inhibiting fatty acid synthase. *Target Oncol*. 2014;9(3):279–286.
30. Lou J, Hu W, Tian R, et al. Optimization and evaluation of a thermo-responsive ophthalmic in situ gel containing curcumin-loaded albumin nanoparticles. *Int J Nanomedicine*. 2014;9:2517–2525.
31. Zhang L, Hou S, Mao S, Wei D, Song X, Lu Y. Uptake of folate-conjugated albumin nanoparticles to the SKOV3 cells. *Int J Pharm*. 2004;287(1–2):155–162.
32. Zhang LK, Hou SX, Zhang JQ, Hu WJ, Wang CY. Preparation, characterization, and in vivo evaluation of mitoxantrone-loaded, folate-conjugated albumin nanoparticles. *Arch Pharm Res*. 2010;33(8):1193–1198.
33. Lu Y, Li J, Wang G. In vitro and in vivo evaluation of mPEG-PLA modified liposomes loaded glycyrrhetinic acid. *Int J Pharm*. 2008;356(1–2):274–281.
34. Cheng M, Xu H, Wang Y, et al. Glycyrrhetinic acid-modified chitosan nanoparticles enhanced the effect of 5-fluorouracil in murine liver cancer model via regulatory T-cells. *Drug Des Devel Ther*. 2013;7:1287–1299.
35. Liu J, Xu H, Zhang Y, et al. Novel tumor-targeting, self-assembling peptide nanofiber as a carrier for effective curcumin delivery. *Int J Nanomedicine*. 2014;9:197–207.